PHYSICAL REVIEW B **69**, 012102 (2004)

Lattice location and stability of implanted Cu in ZnO

U. Wahl, E. Rita, J. G. Correia,* and E. Alves
Instituto Tecnológico e Nuclear, Estrada Nacional 10, PT-2686-953 Sacavém, Portugal

J. G. Soares
Centro de Física Nuclear da Universidade de Lisboa, Avenida Professor Gama Pinto 2, PT-1649-003 Lisboa, Portugal

The ISOLDE Collaboration
CERN-EP, CH-1211 Geneva 23, Switzerland

(Received 8 October 2003; published 14 January 2004)

The lattice location of copper in single-crystalline zinc oxide was studied by means of the emission channeling technique. Following 60-keV room-temperature implantation at a fluence of 2.3×10^{13} cm^{-2}, the angular distribution of β^- particles emitted by the radioactive isotope ^{67}Cu was measured by a position-sensitive detector. The β^- emission patterns give direct evidence that in the as-implanted state a large fraction of Cu atoms (60%–70%) occupy almost ideal substitutional Zn sites with root-mean-square (rms) displacements of 0.16–0.17 Å. However, following annealing at 600 °C and above Cu was found to be located on sites that are characterized by large rms displacements (0.3–0.5 Å) from Zn sites.

DOI: 10.1103/PhysRevB.69.012102 PACS number(s): 61.72.Vv, 61.85.+p

The 3d transition-metal copper is a common impurity in ZnO crystals, and concentrations up to the ppm range have been reported.[1–4] The main interest in Cu results from its possible role in the so-called ''structured'' green luminescence frequently found in ZnO. This role was first suggested by Dingle[1] from an apparent isotope split due to ^{63}Cu and ^{65}Cu in the two no-phonon lines of the structured green luminescence, which has since then often been attributed to $Cu^{2+}_{Zn}(3d^9\,4s^2)$ (Refs. 1–5). ZnO also may exhibit ''unstructured'' green luminescence, and recently Garces *et al.* reported that a 900 °C anneal for 1 h in air transformed the unstructured green luminescence of an as-grown ZnO sample to the structured green ''Cu'' luminescence.[4] They suggested this behavior to be due to Cu being converted from Cu^+ $(3d^{10}\,4s^2)$ to Cu^{2+} $(3d^9\,4s^2)$ by the annealing procedure. However, the role of Cu in the ZnO green luminescence is not undisputed and native defects such as Zn vacancies,[6,7] O antisite defects,[8] or O vacancies[9–11] are being considered as possible candidates, too.

Apart from its possible influence on the optical properties of ZnO, Cu has recently been found a suitable codopant in order to activate room-temperature ferromagnetism in $Zn_{0.94}Fe_{0.05}Cu_{0.01}O$,[12] other applications of Cu in ZnO include varistor[13] and piezoelectric[14] devices. In these three cases the beneficial role of Cu is presumably related to the formation of electrically active Cu acceptors.

While electron paramagnetic resonance experiments have given indirect evidence for the existence of substitutional Cu^{2+}_{Zn} $(3d^9\,4s^2)$ on Zn sites,[15,16] infrared luminescence data point towards the existence of several different Cu defects.[2,5] In addition, resistivity measurements found the conductivity change in Cu-doped ZnO to be roughly proportional to the square of the Cu concentration and were explained by the passivation of Cu_{Zn} acceptors by O vacancies,[17,18] or the formation of acceptor-type Cu^{2+}-Cu^{2+} pairs.[16] So far there are no experiments reported which studied the structural properties of Cu in ZnO in detail. Lattice location methods by means of ion beam channeling and Rutherford backscattering spectroscopy (RBS) are not applicable because Cu has a smaller atomic mass than Zn. Ion beam experiments using particle-induced x-ray emission (PIXE), which were, for instance, used in order to locate Fe in ZnO,[19] are also difficult to perform since Cu and Zn are direct neighbors in the periodic system, and, moreover, such studies would require implanted Cu fluences in the 10^{16} cm^{-2} range. Recently, the extended X-ray absorption fine structure (EXAFS) method has been applied to ZnO samples containing 0.12 at. % Cu, which was incorporated during molecular beam epitaxy growth.[20] This study did only consider ideal substitutional Zn and O sites, and it was found that the EXAFS data resembled Cu on Zn sites but did not completely match the theoretically expected signal. It was also suggested that, depending on the Cu concentration and growth temperature, Cu resides in different structural environments.

We report here on the lattice location of ion-implanted Cu in single-crystalline hexagonal ZnO using the emission channeling technique.[21] For that purpose we have measured the angular distribution of β^- particles emitted by the radioactive isotope ^{67}Cu ($t_{1/2}=61.9$ h). The same method was applied previously in order to investigate the lattice sites of Cu in Si.[22,23]

The ZnO sample studied was a single crystal, grown by seeded chemical vapor transport[24] and polished on the Zn face. Implantation of ^{67}Cu was performed at CERN's on-line isotope separator facility ISOLDE, which provides clean 60-keV beams of Cu from chemically selective laser ion sources. We implanted 7° from the surface normal up to a fluence of 2.3×10^{13} cm^{-2}, leading to a maximum ^{67}Cu concentration of 8×10^{18} cm^{-3} ($\sim$96 ppm) at a depth of 259(116) Å. The angular distribution of β^- particles was recorded by a position-sensitive electron detector and emission channeling patterns were extracted from the energy window 93–577 keV.

In order to identify the lattice sites of Cu, we have fitted the experimental electron distributions by simulated patterns

originating from ^{67}Cu emitter atoms on substitutional Zn sites (S_{Zn}) with varying root-mean-square (rms) displacements u_1. Besides, we also considered substitutional O and a wide range of interstitial sites the location of which has been described in Ref. 25. The electron channeling simulations were carried out by means of the ''many-beam'' formalism[21] using 16 beams, treating the energy range of 100–550 keV in steps of 25 keV and averaging the results according to the β^- spectrum of ^{67}Cu. As described previously in Ref. 26, two models for the crystal structure of ZnO were considered, differing somewhat in the rms displacements of Zn and O atoms and the c-axis bond length parameter. Both models led essentially to the same results for the ^{67}Cu lattice location.

Following room-temperature implantation of ^{67}Cu, the sample was subjected to an annealing sequence up to 800 °C in steps of 100 K under vacuum. The annealing time for each step was 10 min and the relaxation back to room temperature took up to 15 min since the sample could not be quenched in vacuum. Following each annealing step the β^- emission patterns around the [0001], [$\underline{1}$102], [$\underline{1}$101], and [$\underline{2}$113] crystal directions were recorded in order to distinguish between possible substitutional and interstitial sites. Before discussing the results of the complete annealing sequence, we will first focus on the data obtained following the 200 °C (Fig. 1) and 600 °C (Fig. 2) steps. Panels (a)–(d) of Fig. 1 show the channeling patterns measured after the 200 °C annealing, which are essentially the same as in the as-implanted state. The best two-fraction fits of the theoretical yields to the experimental data are shown in Figs. 1(e)–1(h) and give the result that ~70% of Cu atoms occupy substitutional Zn sites. The best fit parameters for the Cu rms displacements from the S_{Zn} sites perpendicular to the [0001], [$\underline{1}$102], [$\underline{1}$101], and [$\underline{2}$113] directions were 0.17 Å, 0.16 Å, 0.16 Å, and 0.15 Å, respectively. While these values are roughly twice as large as the rms displacements of Zn or O atoms (~0.08 Å) (Ref. 27), they are similar to those we have observed for ^{167m}Er implanted in ZnO, though following annealing at the much higher temperature of 700 °C (Ref. 26). The remaining 30% of Cu atoms are attributed to so-called random sites, which are lattice positions resulting in isotropic yield patterns. Allowing for Cu on other than S_{Zn} and random sites did not significantly improve the quality of fit: in particular, we found no indications for Cu on well-defined interstitial sites.

Figures 2(a)–2(d) show the patterns recorded after the 600 °C annealing, which exhibit some characteristic differences compared to the as-implanted or 200 °C-annealed data. Not only is the general anisotropy roughly reduced by a factor of 2, but also the relative intensity of the axial channeling effects greatly diminished with respect to the planar channeling effects. In the case of the [0001] pattern, there is even a local minimum visible along the axial direction. These changes are clear indications that the preferential lattice position of Cu has altered. Indeed, the best fit was now obtained for ~95% of Cu on S_{Zn} sites with the large rms displacements of 0.42 Å, 0.44 Å, 0.44 Å, and 0.46 Å, respectively. Such large u_1 values are likely to be caused by static displacements along specific crystal directions. We have therefore also tried to fit the data with sites that are

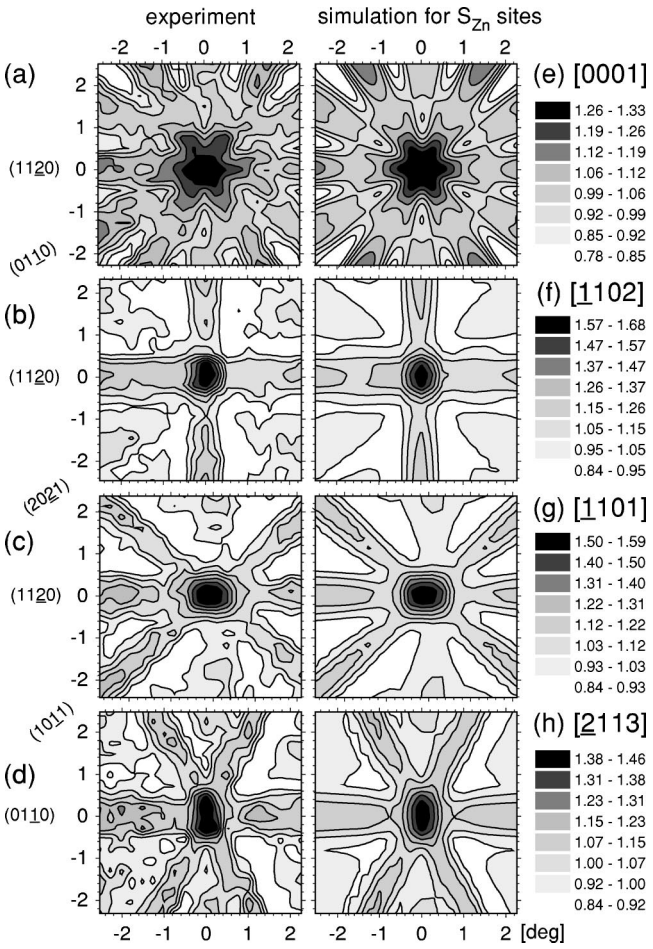

FIG. 1. Angle-dependent β^- emission yields from ^{67}Cu-implanted ZnO around the [0001] (a), [$\underline{1}$102] (b), [$\underline{1}$101] (c), and [$\underline{2}$113] (d) axes following annealing at 200 °C. Panels (e)–(h): best fits of simulated channeling patterns to the experimental yields, corresponding to 73%, 68%, 71%, and 65% of Cu on S_{Zn} sites with rms displacements of 0.17 Å, 0.16 Å, 0.16 Å, and 0.15 Å, respectively.

shifted along the c axis or along the basal bonding and antibonding directions. However, sufficiently good fits were obtained for isotropic Gaussian distributions around the substitutional Zn sites and it was not possible to relate the displacement with specific directions.

In Fig. 3 we have compiled the Cu fractions on S_{Zn} sites and the rms displacements u_1 from the perfect substitutional Zn positions following the different annealing steps. Following annealing to 400 °C, the fraction of Cu on S_{Zn} sites remained essentially the same as following 200 °C annealing while u_1 already increased somewhat to values between 0.22 Å and 0.26 Å. Annealing at 600 °C led to a pronounced increase of the rms displacements. Finally, following annealing at 700 and 800 °C, the rms displacements remained at rather high values while the apparent S_{Zn}-related fraction of Cu decreased. On dismounting the crystal from the vacuum chamber several percent of the ^{67}Cu activity was found outside the sample, giving direct evidence that, at least during the last annealing step, significant diffusion of Cu occurred. Möller and Helbig have reported a diffusion coefficient of

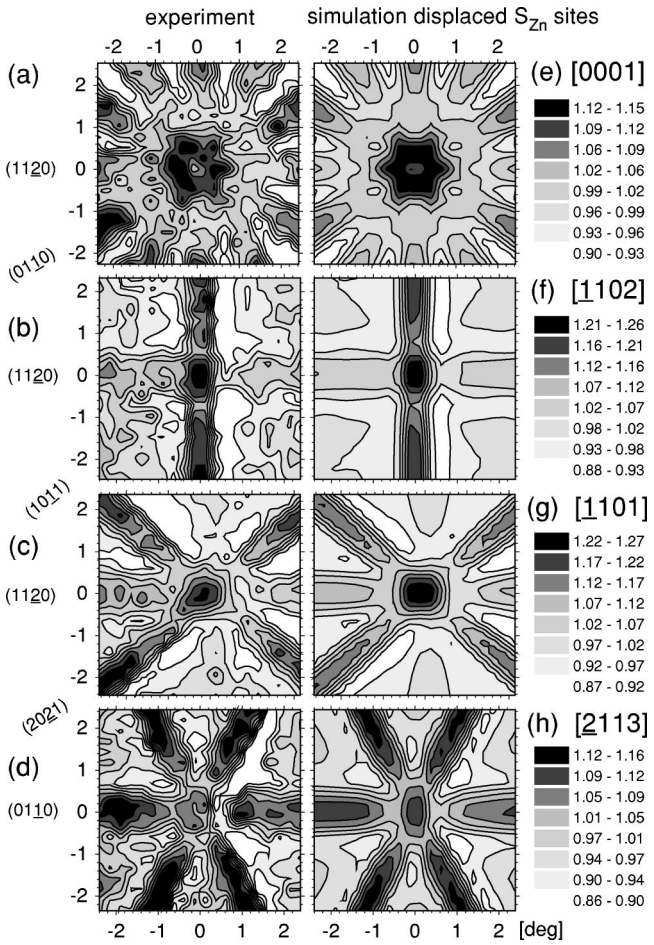

FIG. 2. β^- emission channeling patterns around the [0001] (a), [$\bar{1}$102] (b), [$\bar{1}$101] (c), and [$\bar{2}$113] (d) axes following annealing at 600 °C. Panels (e)–(h): best fits, corresponding to 85%, 100%, 106%, and 87% of Cu on S_{Zn} sites with rms displacements of 0.42 Å, 0.44 Å, 0.44 Å, and 0.46 Å, respectively.

$D=2\times10^7$ exp(−4.8 eV/kT) cm^2/s for Cu in ZnO.[16] For our 10-min annealing at 800 °C this would imply a diffusion width around 60 Å. While this compares to the mean implantation depth of 259 Å we note that the changes in the configuration of substitutional Cu start already around 400 °C. Some remarks are also appropriate on the possible influence of the Cu diffusion on the accuracy of the lattice location results. Emission channeling effects generally decrease with increasing depth of the emitter atoms from the surface due to dechanneling. The fitted fractions are therefore quite sensitive to the Cu depth profile, and while our simulations assumed an as-implanted profile, the diffusion obviously must have caused changes in the Cu depth distribution. In Fig. 3(a) we have therefore marked the ^{67}Cu fractions for annealing temperatures at 600 °C and above as less accurate. The apparent increase of the fraction of near-substitutional Cu to 95% following 600 °C and its reduction following 700 and 800 °C annealing are possibly simply reflecting changes in the Cu depth profile. In contrast, the derived Cu rms displacements hardly depend on its depth profile. We have verified this by also comparing the experimental data to simulations using a constant ^{67}Cu depth profile from 0 to 5000 Å.

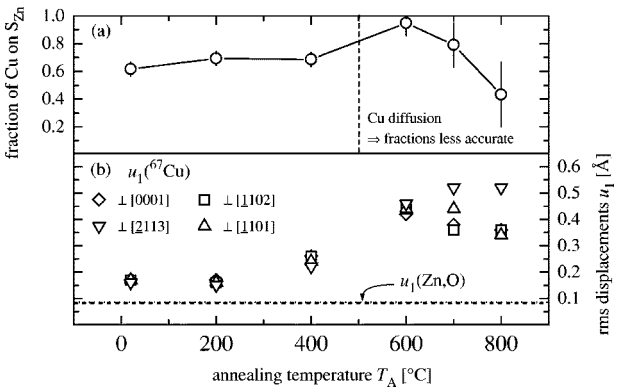

FIG. 3. Fraction of Cu atoms on substitutional Zn sites (a) and their room-temperature rms displacements $u_1(^{67}\mathrm{Cu})$ perpendicular to the indicated crystal directions (b) following 10-min annealing steps. Zn and O rms displacements (Ref. 27) are also indicated.

In this case, while the hypothetical fitted fractions would exceed 500%, the best fit values for $u_1(^{67}\mathrm{Cu})$ would still be around 0.42–0.52 Å.

We would like to add some remarks regarding the consequences of thermal annealing on Cu in ZnO. We note that both our results and those of Ref. 16 imply that substantial diffusion of Cu must take place during 900 °C annealing. Pronounced diffusion, however, offers ample possibilities of Cu atoms being trapped by various sorts of defects. Hence, the Cu sites following high-temperature annealing are therefore likely to represent Cu in complexes with additional defects (these could be native defects such as vacancies and interstitials or other impurities) or, possibly, Cu_{Zn}-Cu_{Zn} pairs. The formation of these complexes should depend on the concentration of Cu and the other constituents, and on the conditions of annealing, such as temperature, duration, slow cool-down, or quench, annealing atmosphere (Zn-rich or O-rich). Our findings do not completely rule out the possibility that the structured green luminescence observed following 900 °C annealing[4] is due to Cu on ideal substitutional Zn sites (these sites could be occupied again under different experimental conditions—for instance, during a fast quench or for annealing under different atmospheres). However, the fact that the simple substitutional Cu_{Zn} defect does not easily survive high-temperature annealing provides additional evidence that other Cu-related centers or entirely different defects not involving Cu are in fact responsible for the structured green luminescence.

Summarizing, we have identified two configurations of implanted Cu in ZnO. In the as-implanted state, Cu is mainly found on almost ideal S_{Zn} sites, characterized by small rms displacements around 0.15–0.17 Å. However, this configuration of Cu has low thermal stability, and vacuum annealing at 400 °C starts the conversion of Cu from almost ideal Zn sites to Zn sites with large displacements, of the order of 0.35–0.50 Å. Finally, annealing at 800 °C in vacuum leads to partial Cu outdiffusion.

This work was funded by the FCT, Portugal (Project No. CERN/FIS/43725/2001) and by the European Union (Large Scale Facility Contract No. HPRI-CT-1999-00018). U.W. and E.R. acknowledge support by the FCT, Portugal.

*On leave at CERN-EP, CH-1211 Geneva 23, Switzerland.
[1] R. Dingle, Phys. Rev. Lett. **23**, 579 (1969).
[2] H.J. Schulz and M. Thiede, Phys. Rev. B **35**, 18 (1987).
[3] P. Dahan, V. Fleurov, P. Thurian, R. Heitz, A. Hoffmann, and I. Broser, J. Phys.: Condens. Matter **10**, 2007 (1998).
[4] N.Y. Garces, L. Wang, L. Bai, N.C. Giles, L.E. Halliburton, and G. Cantwell, Appl. Phys. Lett. **81**, 622 (2002).
[5] P.J. Dean, D.J. Robbins, S.G. Bishop, J.A. Savage, and P. Porteous, J. Phys. C **14**, 2847 (1981).
[6] A.F. Kohan, G. Ceder, D. Morgan, and C.G. Van De Walle, Phys. Rev. B **61**, 15 019 (2000).
[7] D.C. Reynolds, D.C. Look, and B. Jogai, J. Appl. Phys. **89**, 6189 (2001).
[8] B. Lin, Z. Fu, and Y. Jia, Appl. Phys. Lett. **79**, 943 (2001).
[9] K. Vanheusden, W.L. Warren, C.H. Seager, D.R. Tallant, J.A. Voigt, and B.E. Gnade, J. Appl. Phys. **79**, 7983 (1996).
[10] X.L. Wu, G.G. Siu, C.L. Fu, and H.C. Ong, Appl. Phys. Lett. **78**, 2285 (2001).
[11] S.B. Zhang, S.H. Wei, and A. Zunger, Phys. Rev. B **63**, 075205 (2001).
[12] S.J. Han, J.W. Song, C.H. Yang, S.H. Park, J.H. Park, Y.H. Yeong, and K.W. Rhie, Appl. Phys. Lett. **81**, 4212 (2002).
[13] T.R.N. Kutty and N. Raghu, Appl. Phys. Lett. **54**, 1796 (1989).
[14] J.B. Lee, H.J. Lee, S.H. Seo, and J.S. Park, Thin Solid Films **398**, 641 (2001).
[15] R.E. Dietz, H. Kamimura, M.D. Sturge, and A. Yariv, Phys. Rev. **132**, 1559 (1963).
[16] G. Müller and R. Helbig, J. Phys. Chem. Solids **32**, 1971 (1971).
[17] G. Bogner and E. Mollwo, J. Phys. Chem. Solids **6**, 136 (1957).
[18] G. Bogner, J. Phys. Chem. Solids **19**, 235 (1961).
[19] T. Monteiro, C. Boemare, M.J. Soares, E. Rita, and E. Alves, J. Appl. Phys. **93**, 8995 (2003).
[20] P. Fons, A. Yamada, K. Iwata, K. Matsubara, S. Niki, K. Nakahara, and H. Takasu, Nucl. Instrum. Methods Phys. Res. B **199**, 190 (2003).
[21] H. Hofsäss and G. Lindner, Phys. Rep. **210**, 121 (1991).
[22] U. Wahl, A. Vantomme, G. Langouche, J.G. Correia, and the ISOLDE Collaboration, Phys. Rev. Lett. **84**, 1495 (2000).
[23] U. Wahl, A. Vantomme, G. Langouche, J.P. Araújo, L. Peralta, J.G. Correia, and the ISOLDE Collaboration, Appl. Phys. Lett. **77**, 2142 (2000).
[24] Eagle-Picher Technologies, Miami, OK 74354.
[25] U. Wahl, A. Vantomme, G. Langouche, J.P. Araújo, L. Peralta, and L.G. Correia, J. Appl. Phys. **88**, 1319 (2000).
[26] U. Wahl, E. Rita, J.G. Correia, E. Alves, J.P. Araújo, and the ISOLDE Collaboration, Appl. Phys. Lett. **82**, 1173 (2003).
[27] A. Yoshiasa, K. Koto, H. Maeda, and T. Ishii, Jpn. J. Appl. Phys., Part 1 **36**, 781 (1997).